On the application of scintillometry over heterogeneous grids

J. Ezzahar, Ghani Chehbouni, Joost Hoedjes, Ah Chehbouni

Journal of Hydrology (2006) xxx, xxx–xxx

available at www.sciencedirect.com

ScienceDirect

journal homepage: www.elsevier.com/locate/jhydrol

On the application of scintillometry over heterogeneous grids ☆

J. Ezzahar [a], A. Chehbouni [b,*], J.C.B. Hoedjes [b], Ah. Chehbouni [a]

[a] Physics Department LMFE, Faculty of Sciences Semlalia, Marrakech, Morocco
[b] Centre d'Etudes Spatiales de la Biosphère (CESBIO), 18 Avenue Edouard Belin, 31401 Toulouse Cedex 9, France

Received 2 December 2005; received in revised form 13 October 2006; accepted 20 October 2006

KEYWORDS
Scintillation;
Eddy covariance;
Heterogeneity;
Aggregation;
Structure parameter

Summary In this paper the applicability of the Monin–Obukhov similarity theory (MOST) over heterogeneous terrain below the blending height is investigated. This is tested using two large aperture scintillometers (LAS), in conjunction with aggregation schemes to infer area-averaged refractive index structure parameters. The two LAS were operated simultaneously over the oliveyard of Agdal, located near Marrakech (Morocco). The Agdal olive yard is made up of two contrasted fields, or patches. The two sites are relatively homogeneous, but differ strongly in characteristics (mainly soil moisture status, and, to a lesser extent, vegetation cover). The higher soil moisture in the northern site creates heterogeneity at the scale of the entire olive yard (i.e. at grid scale). At patch scale, despite the complexity of the surface (tall, sparse trees), a good agreement was found between the sensible heat fluxes obtained from eddy-covariance systems and those estimated from the LAS. At grid scale, the aggregated structure parameter of the refractive index, simulated using the proposed aggregation model, behaves according to MOST. This aggregated structure parameter of the refractive index is obtained from measurements made below the grid scale blending height, and shows that MOST applies here. Consequently, scintillometers can be used at levels below the blending height. This is of interest, since strictly respecting the height requirements poses tremendous practical problems, especially if one is aiming to derive surface fluxes over large areas.

Introduction

The structure parameter of the refractive index (C_n^2) of air is a key parameter that characterizes the intensity of the turbulent fluctuations of the atmospheric refractive index. Using the scintillation technique, one can measure this parameter at spatial scales varying from several hundreds

☆ We, the authors, declare that the presented paper contains original work, is not being submitted elsewhere, and all authors agree to the contents and submission of the paper.

* Corresponding author. Tel.: +33 561 558 197; fax: +33 561 558 500.
E-mail address: ghani@cesbio.cnes.fr (A. Chehbouni).

0022-1694/$ - see front matter © 2006 Published by Elsevier B.V.
doi:10.1016/j.jhydrol.2006.10.027

of meters (e.g. displaced-beam laser scintillometer) up to 10 km (e.g. extra large aperture scintillometer). Depending on the wavelength at which the scintillometer operates, knowledge of C_n^2 permits the calculation of vertical fluxes of heat or water vapour from the earth's surface, which are required in many meteorological, hydrological and agricultural applications. These fluxes can be, and have been, measured using point-sampling measurement devices such as Bowen-ratio or eddy-covariance (EC) systems. However, for several applications, in particular large scale irrigation management or the validation of surface parameterization schemes in large-scale hydro-atmospheric models, grid-scale values are required. A network of point-sampling devices, such as eddy-covariance, can be used. However, the high cost and the requirement of continuous availability of well-trained staff to operate and maintain them has led the scientific community to look for alternative techniques to estimate area-averaged fluxes over large heterogeneous surfaces.

In this context, a number of different techniques have been introduced for research applications, such as a dispersometer theodolite, displaced-beam laser scintillometers, microwave scintillometers and large or extra large aperture scintillometers (LAS, XLAS). In this study we focus on the scintillation technique. The principle of scintillometry consists of transmitting a beam of electromagnetic radiation and measuring the intensity variations of the received signal. Wang et al. (1978) have shown that the variance of the logarithm of the intensity fluctuations can be related to C_n^2, which, for scintillometers operating at visible or near-infrared wavelengths, can then be related to the structure parameter of temperature, C_T^2, to derive the sensible heat flux through Monin–Obukhov similarity theory (MOST) (Wesely, 1976; Moene, 2003). Due to its ability to integrate atmospheric processes along a transect, varying from a few hundreds of metres up to a several kilometres, the scintillation method is a promising approach for routine observations of surface fluxes. Compared to e.g. eddy-covariance systems, the scintillometer is easy to install, relatively cheap and it is a practical method to obtain area-average surface fluxes over several kilometres. The instrument is capable of continuous measurements with minimum human intervention.

Over the last decade, several authors have proven the reliability of heat flux estimates from scintillometer over fairly homogeneous terrain (e.g. Green et al., 1994; de Bruin et al., 1995; Meijninger and de Bruin, 2000; Hoedjes et al., 2002). Recently, several investigations have demonstrated the potential of this method over moderately inhomogeneous surfaces (Chehbouni et al., 1999, 2000b; Beyrich et al., 2002; Meijninger et al., 2002). However, a disadvantage of the method is that it requires the use the semi-empirical Monin–Obukhov similarity theory which might not be applicable over very complex surfaces (Lagouarde et al., 2002).

The main objective of this paper is to test the applicability of MOST at grid scale. The grid consists of two or more distinct fields (or patches) with different characteristics, creating a heterogeneous (grid) surface. This is tested by combining LAS measurements, over two individually homogeneous patches with different characteristics, with aggregation schemes to derive a grid scale average refractive index structure parameter, $\langle C_n^2 \rangle$ (angular brackets denoting grid scale averages). The aggregation scheme is required since C_n^2 is not linear. Regarding the aggregation issue, we have adopted the deterministic approach (Shuttleworth, 1991; Arain et al., 1996; Noilhan and Lacarrere, 1995; Chehbouni et al., 1995, 2000a; Lagouarde et al., 2002), which consists of deriving analytical relationships between local and effective (area-averaged) surface parameters by matching the model equations at different scales. In order to develop the aggregation scheme and to verify the applicability of the Monin–Obukhov similarity theory (MOST), a field experiment has been designed and carried out during the autumn of 2002 over the olive yard of Agdal in Morocco, within the framework of the SUDMED (Chehbouni et al., 2003) and IRRIMED projects (http://www.irrimed.org).

This paper is organized as follows: in ''Theoretical background'' section, the basic equations and the associated procedure that allow the estimation of sensible heat flux from the structure parameter of the refractive index of air are presented. An overview of the experimental design is outlined in ''Experimental site and measurements'' section. In ''Aggregation procedures for obtaining grid averaged C_n^2'' section, we present the developed aggregation scheme to derive the area-averaged refractive index structure parameter $\langle C_n^2 \rangle$ over two adjacent olive tree fields under unstable conditions. In ''Results and discussion'' section, a comparison between LAS and EC derived measurements at both patch and at grid scales is presented (where patch scale refers to individual fields and grid scale to the ensemble of several (in our case two) fields). Finally, we conclude by discussing the accuracy of the suggested approach to estimate the area-averaged structure parameter of the refractive index and the applicability of MOST at grid scale using measurements made below the blending height.

Theoretical background

The large aperture scintillometer (LAS) is a device that measures the structure parameter of the refractive index of air. In the optical domain, this C_n^2 depends mainly on temperature fluctuations and, to a lesser effect, humidity fluctuations. Assuming that temperature and humidity fluctuations are perfectly correlated, Wesely (1976) showed that, to a good approximation, the temperature structure parameter C_T^2 can be derived from C_n^2 by:

$$C_T^2 = C_n^2 \left(\frac{T^2}{\gamma p}\right)^2 \left(1 + \frac{0.03}{\beta}\right)^{-2}, \quad (1)$$

where γ is the refractive index coefficient for air (7.8×10^{-7} K Pa^{-1}), and β the Bowen ratio. The final bracketed term is a correction for the effects of humidity. C_n^2 and C_T^2 are in (m$^{-2/3}$) and (K^2 m$^{-2/3}$), respectively.

According to MOST, it is possible to link C_T^2 and the temperature scale T_* for unstable conditions, i.e., $L < 0$ (de Bruin et al., 1993) using:

$$\frac{C_T^2}{T_*^2 (z-d)^{-2/3}} = f((z-d)/L) = 4.9(1 - 9(z-d)/L)^{-2/3}, \quad (2)$$

L is the Monin–Obukhov length defined as:

Please cite this article in press as: Ezzahar, J et al., On the application of scintillometry ..., J Hydrol. (2006), doi:10.1016/j.jhydrol.2006.10.027

$$L = -\frac{T_a u_*^2}{\kappa g T_*} \quad (3)$$

with $\kappa = 0.41$, $g = 9.81\ \mathrm{m\ s^{-2}}$ and u_* is the friction velocity, given by:

$$u_* = \kappa u[\ln((z-d)/z_0) - \psi((z-d)/L)]^{-1}, \quad (4)$$

where ψ is the integrated stability function (Panofsky and Dutton, 1984), z is the measurement height, d the displacement height and z_0 is the roughness length.

The sensible heat flux H ($\mathrm{W\ m^{-2}}$) is calculated iteratively using Eqs. (1)–(4) and the following relationship:

$$H = \rho c_p u_* T_*, \quad (5)$$

where ρ ($\mathrm{kg\ m^{-3}}$) and c_p ($\mathrm{J\ kg^{-1}\ K^{-1}}$) are the air density and specific heat capacity at constant pressure, respectively.

Experimental site and measurements

The experiment was carried out in the fall of 2002, between day of year (DOY) 295 and 306 (22nd October–2nd November) at the 275 ha Agdal olive orchard, which is located to the southeast of the city of Marrakech, Morocco (31°36′N, 07°59′W). The climate is semiarid Mediterranean. Precipitation falls mainly during winter and spring, from the beginning of November until the end of April, with an average yearly rainfall of 175–250 mm. The atmosphere is very dry, with an average humidity of 50%, and the potential evaporation is very high (1600 mm per year), greatly exceeding the annual rainfall. The experimental area is divided in two fields, which are referred to as the southern site and the northern site. The average height of the olive trees is 6.5 m in the southern and 6 m in the northern site. The vegetation is more homogenous in the southern site than in the northern site, as can be seen in Fig. 1, with an average vegetation cover of approximately 55% in the southern site and 45% in the northern site, as obtained from hemispherical canopy photograhps (using a Nikon Coolpix 950® with a FC-E8 fish-eye lens converter, field of view 183°). The period of the experiment was chosen in order to have a distinct difference between the two sites in term of soil moisture. The southern site was dry and the northern site had just been irrigated. Fig. 2 shows the evolution of the volumetric water content throughout the experiment. From Fig. 2, it is clear that the grid, comprised of the northern and southern sites, is heterogeneous.

Both sites were equipped with a set of standard meteorological instruments to measure wind speed and direction (Young Wp200) and air temperature and humidity, using HMP45AC temperature and humidity probes (Vaisala) at 9 m. Furthermore, net radiation in the southern site was measured using a CNR1 (Kipp and Zonen) installed at 8 m and Q7 net radiometer (REBS) at 7 m. In the northern site the net radiation was measured with a Q6 net radiometer (REBS) at 8 m. Net radiation over the soil in both fields was measured by a Q7 at 1 m. Soil heat flux was measured at three locations at a depth of 0.01 m using soil heat flux plates (Hukseflux). The first was located below the canopy close to the trunk of a tree, in order to be not exposed to solar radiation; the second was exposed directly to solar radiation, and the third was installed in an intermediate position, partly sunlit, partly shaded. An average of these three measurements was calculated to obtain a representative value. Soil moisture was measured at different depths (0.05, 0.1, 0.2, 0.3 and 0.4 m) using 5 CS616 water content reflectometers (Campbell Scientific Ltd.). All meteorological measurements were sampled at 1 Hz, and 30 min averages were stored. The prevailing wind direction is from the northwest.

In both the northern and the southern site, EC systems were installed to provide continuous measurements of the vertical fluxes of heat, water vapour and CO_2 at a height of 8.8 and 8.7 m for the southern and northern sites, respectively. The EC systems consisted of a 3D sonic anemometer (CSAT3, Campbell Scientific Ltd.) and an open-path infrared gaz analyzer (Li7500, Licor Inc.). Raw data were sampled at a rate of 20 Hz and were recorded using CR23X dataloggers (Campbell Scientific Ltd.) which were connected to portable computers to enable storage of large raw data files. The half-hourly values of fluxes were later calculated off-line after performing coordinate rotation, frequency corrections, correcting the sonic temperature for the lateral velocity and presence of humidity, and the inclusion of the mean vertical velocity according to Webb et al. (1980). Data from the eddy-covariance system were processed using the software 'ECpack' developed by the Meteorology and Air Quality group, Wageningen University (available for download at http://www.met.wau.nl/).

Air pressure was measured in the southern site using the pressure sensor of the Li7500 infrared gas analyzer, and on the northern site using a pressure sensor (Vaisala PTB101B). 1 min averages were recorded on the dataloggers.

The LAS operated in this study were built by the Meteorology and Air Quality Group (Wageningen University, the Netherlands). These instruments have been constructed according to the basic design described in Ochs and Wilson (1993). They have an aperture size of 0.15 m and the transmitter operates at a wavelength of 0.94 μm. At the receiver, C_n^2 is sampled at 1 Hz and averaged over 1 min intervals by a CR510 datalogger. Two identical LAS were used in this experiment. The first was installed over the southern site, perpendicular to the dominant wind direction, over a pathlength of 1050 m (denoted LAS_S). The transmitter was mounted on a tripod installed on a roof, located on the southwest corner of the southern site, while the receiver was mounted on a 15 m high tower that was positioned next to the road that separates the two sides of the orchard. The second LAS was installed over the northern site, the orientation of this LAS was almost parallel to the dominant wind direction, and it measured over a pathlength of 1070 m (denoted LAS_N). The receiver was installed on the same tower as the receiver of LAS_S. The transmitter was mounted on a tripod installed on a roof located near the northern corner of the northern site. The setup of the receivers on the 15 m tower was such that the two signals did not interfere. The average heights of the LAS transects were 14 m for the southern site and 14.5 m for the northern site.

From Fig. 1 it can be seen that the two experimental sites, especially the northern site, are not completely homogeneous; intersecting dirt roads and missing trees cause a certain degree of heterogeneity. However, considering the horizontal scale of these heterogeneities, the experimental setup of both the EC systems and the LAS

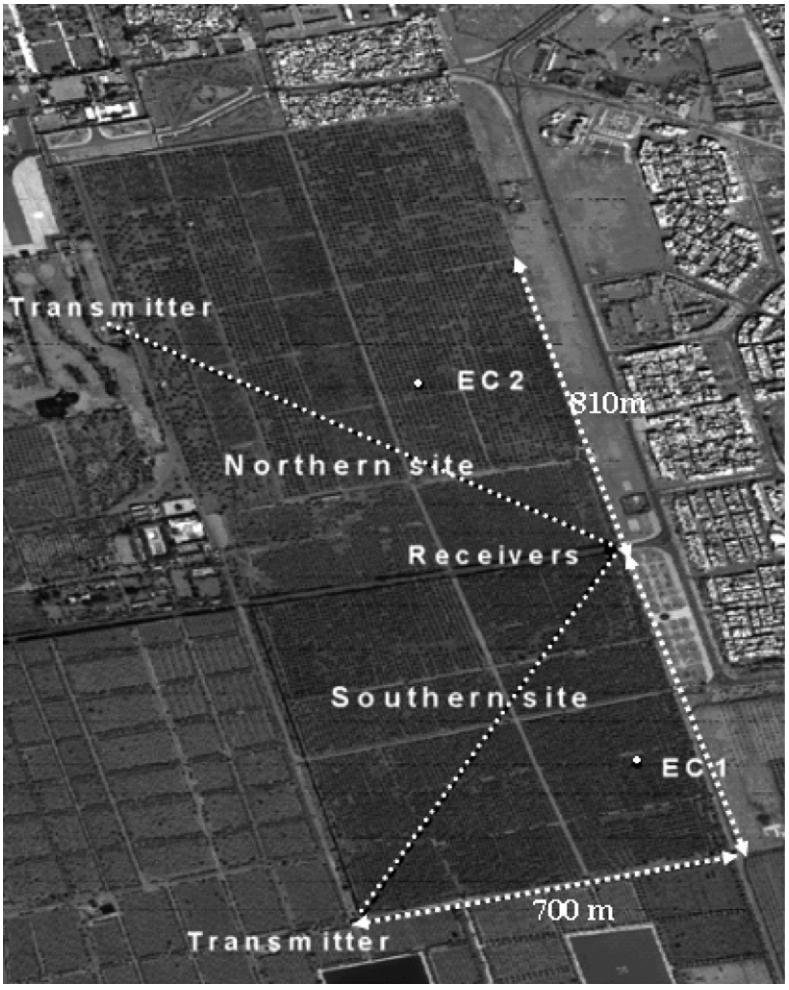

Figure 1 Overview of the experimental site (Quickbird image).

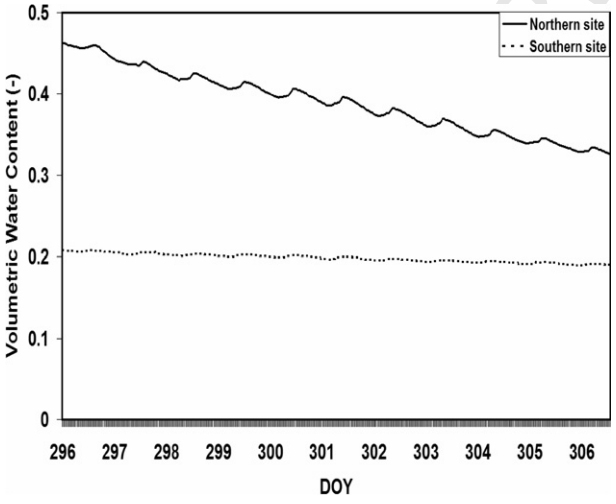

Figure 2 Evolution of the volumetric water content during the experimental period for the southern site (dotted line) and northern site (solid line).

are believed to be at or above the blending height, or the height at which the turbulent signatures of the individual heterogeneous structures are mixed, and above which MOST is generally accepted to be applicable (Meijninger et al., 2002). In this study, *patch scale* refers to either northern or southern site, whereas *grid scale* refers to the entire oliveyard (or, the ensemble of northern and southern sites).

Aggregation procedures for obtaining grid averaged C_n^2

Due to the non-linearity of C_n^2, the grid-scale average refractive index structure parameter $\langle C_n^2 \rangle$ cannot be obtained as a weighted average of the patch-scale C_n^2 values. Two alternative approaches are described in this section: the effective approach (denoted by subscript 'eff') and the aggregational approach (denoted by subscript 'agg'). In the effective approach, values of $\langle C_n^2 \rangle_{\text{eff}}$ are obtained through the combination of eddy correlation based measurements of H, L_vE, and u_* and MOST, In the aggregated approach, $\langle C_n^2 \rangle_{\text{agg}}$ is obtained through a combination of MOST, an aggregation scheme and the LAS-based patch-scale measurements of C_n^2.

Effective approach

The effective approach consists of deriving an area-averaged C_n^2 from eddy-covariance measurements. This $\langle C_{n\ \text{EC}}^2 \rangle_{\text{eff}}$ is obtained by inverting Eqs. (1)–(5) using grid

scale averages of sensible and latent heat fluxes and friction velocity. $\langle H_{EC}\rangle_{eff}$ and $\langle LvE_{EC}\rangle_{eff}$ are obtained as a simple linear weighted average of the fluxes measured at both sites. The effective friction velocity, $\langle u_{*EC}\rangle_{eff}$, is obtained by applying the matching rule to momentum fluxes (Chehbouni et al., 1999):

$$\langle u_{*EC}\rangle_{eff} = \left(\sum f_{iEC} u_{*iEC}^2\right)^{0.5}, \quad (6)$$

where f_{iEC} is the fraction of the surface covered by the patch i. Since the eddy-covariance systems at both northern and southern sites were installed at approximately the same height above the vegetation, we found it safe to assume $f_{iEC} = 0.5$, since the size of the area from which the measured flux emanates will be roughly the same for each site.

Aggregational approach

The second approach consists of estimating a grid scale average C_n^2 from the LAS measurements. This $\langle C_{nLAS}^2\rangle_{agg}$ is obtained using C_{nS}^2 and C_{nN}^2 in combination with the aggregation scheme described in this section. After obtaining a patch scale sensible heat flux from each LAS (using Eqs. (1)–(5)), a grid-scale sensible heat flux can be obtained as follows:

$$\langle H\rangle = f_c H_{LAS\_S} + (1 - f_c) H_{LAS\_N}, \quad (7)$$

where subscripts S and N indicate variables associated with the southern or northern site, respectively, and f_c is the fraction of the southern area in the entire grid surface. The value of f_c is further discussed in ''grid scale'' section Eqs. (6) and (7) can be simplified as:

$$\langle u_* T_*\rangle = f_c u_{*S} T_{*S} + (1 - f_c) u_{*N} T_{*N}, \quad (8)$$

$$\langle u_*^2\rangle = f_c u_{*S}^2 + (1 - f_c) u_{*N}^2. \quad (9)$$

According to Monin–Obukhov similarity theory and using the scaling constants found by de Bruin et al. (1993):

$$\frac{C_T^2 (z-d)^{2/3}}{T_*^2} = 4.9\left(1 - 9\frac{(z-d)}{L}\right)^{-2/3}. \quad (10)$$

By substituting Eq. (1) into Eq. (10) and Eq. (10) into (8), Eq. (11) can be obtained:

$$\langle C_{nLAS}^2\rangle_{agg} = \langle y\rangle^{-1}(y_S C_{nS}^2 + y_N C_{nN}^2) \quad (11)$$

with:

$$y_X = (f_X)\frac{u_{*X}\left(1 + \frac{0.03}{\beta_X}\right)^{-2}(z_X - d_X)^{2/3}}{T_{*X}\left(1 - 9\frac{(z_X - d_X)}{L_X}\right)^{-2/3}}, \quad (12)$$

where X is either S, N or indicating the grid-scale average (angular brackets), and $f_X = 1$ for $\langle y\rangle$, $f_X = f_c$ for y_S and $f_X = (1 - f_c)$ for y_N. Using once again the principle that consists of formulating grid-scale surface fluxes using the same equations that govern the patch-scale behaviour, but whose arguments are the aggregate expressions of those at the patch-scale (Chehbouni et al., 2000a), $\langle L\rangle$ is derived from the area-average sensible heat flux and friction velocity as :

$$\langle L\rangle = \frac{-\rho c_p T_a \langle u_*\rangle^3}{kg\langle H\rangle}, \quad (13)$$

$\langle\beta\rangle$is the grid-scale average Bowen ratio, defined as:

$$\langle\beta\rangle = \frac{\langle H\rangle}{\langle LvE\rangle}, \quad (14)$$

where $\langle LvE\rangle$ is defined analogous to $\langle H\rangle$ in Eq. (7), with patch scale values of LvE obtained as the resultant of the energy balance ($LvE_{LAS} = R_n - G - H_{LAS}$).

On the other hand, one should mention that aggregation procedures based on the flux matching rules do not deal directly with the primary surface variables, such as roughness length and displacement height. In this context, and according to previous study (Shuttleworth, 1988; Lagouarde et al., 2002), a semi-empirical approach is generally used. It stipulates that ''the effective area-average value of land surface parameters is estimated as a weighted average over the component cover types in each grid through that function involving the parameter which most succinctly expresses its relationship with the associated surface flux''. Subsequently, in this context, the grid scale average displacement height, $\langle d\rangle$, and roughness length, $\langle z_0\rangle$, are expressed as:

$$\langle d\rangle = f_c d_S + (1 - f_c) d_N \quad (15)$$

and

$$\left(\ln\left(\frac{z - \langle d\rangle}{\langle z_0\rangle}\right)\right)^{-2} = f_c\left(\ln\left(\frac{z - d_S}{z_{0S}}\right)\right)^{-2} + (1 - f_c) \times \left(\ln\left(\frac{z - d_N}{z_{0N}}\right)\right)^{-2}. \quad (16)$$

Here z_{0S} and z_{0N} represent the roughness length for the southern and northern sites, respectively, each of which is estimated as a fraction of the vegetation height (rule of thumb).

Results and discussion

In this section, the closure of the energy balance of the eddy-covariance data is analysed, followed by a comparison between sensible heat fluxes measured by the EC systems and by the LAS at patch scale. Thereafter we test the applicability of MOST at grid scale when measurements are made below the so-called blending height, followed by a comparison of $\langle C_{nLAS}^2\rangle_{agg}$ and $\langle C_{nEC}^2\rangle_{eff}$ as well as a comparison between the LAS based and EC-based area-averaged sensible heat flux. Note that only unstable conditions ($\frac{(z-d)}{L} < 0$) are considered in this study.

Energy balance closure

As a measure of how the energy balance was closed in our observations, the sum of the latent (LvE) and sensible (H) heat fluxes derived from the EC system is balanced by the available energy (net radiation (R_n) minus soil heat flux (G)). The energy balance closure depends both on the eddy-covariance measurements and the ability to adequately quantify the available energy over an area representative of the flux source area. Most results in the literature have shown the sum of sensible and latent heat fluxes measured by eddy-covariance to underestimate the available energy (Twine et al., 2000; Hoedjes et al., 2002; Testi et al., 2003).

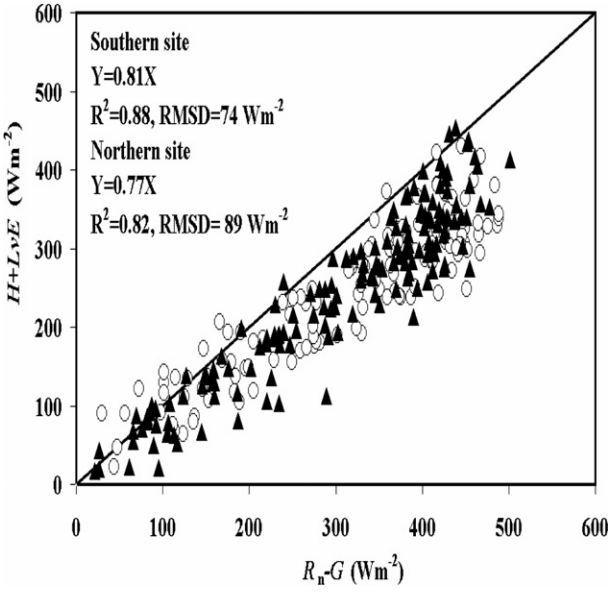

Figure 3 Comparison of half-hourly values of $H + L_vE$ and $R_n - G$ under unstable conditions, for northern site (triangles) and southern site (circles).

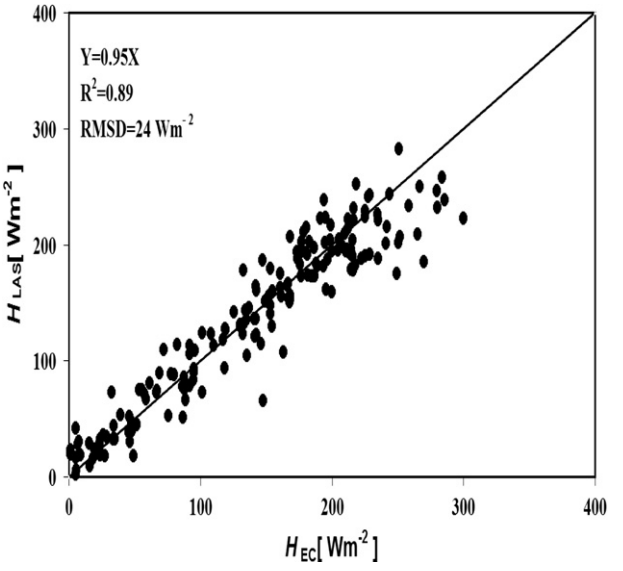

Figure 4a Comparison of H_{LAS} and H_{EC} during unstable conditions for the southern site.

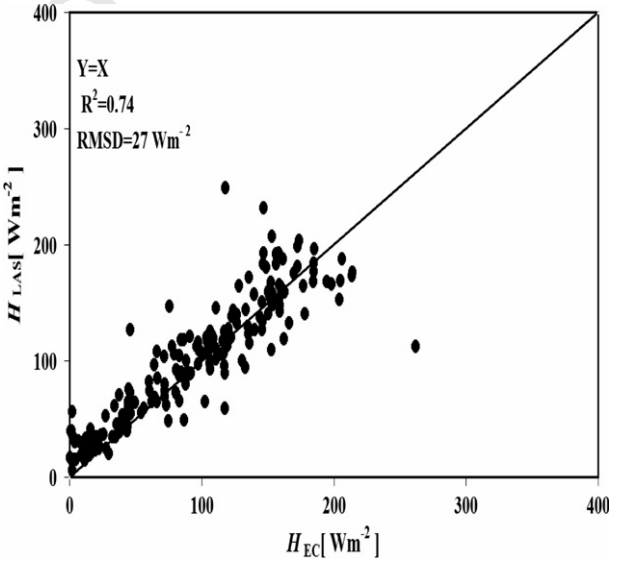

Figure 4b Comparison of H_{LAS} and H_{EC} during unstable conditions for the northern site.

Fig. 3 shows the plots of $R_n - G$ against $H + L_vE$ for the southern and northern sites. The linear regression (forced trough the origin) yields (W m^{-2}) $H_S + LvE_S = 0.81(R_{nS} - G_S)$, $R^2 = 0.88$ and the root mean square difference (RMSD) = 74 W m^{-2} for the southern site, and $H_N + L_vE_N = 0.77(R_{nN} - G_N)$, $R^2 = 0.82$ and RMSD = 89 W m^{-2} for the northern site. Several reasons can be suggested to explain the lack of energy balance closure, for example underestimation of the fluxes measured with the eddy-covariance system, which might be due to the attenuation of the true turbulent signals at sufficiently high and low frequencies (e.g., Moore, 1986) or the differences in source area for convective fluxes and available energy. Additionally, energy storage within the olive tree biomass and in the air column beneath the net radiation measurement is not included in the energy balance. Scott et al. (2003) estimated the energy storage within the biomass in similar ecosystems to be about 5–10% of the available energy, which might explain some of the lack in energy balance closure. However, when compared to results reported in other experimental studies (the average error in closure ranges from 10% to 30% according to Twine et al., 2000), the energy balance closure obtained here can be considered acceptable.

Patch scale

In Figs. 4a and 4b the sensible heat fluxes obtained from the LAS (H_{LAS}) are compared, under unstable conditions, to those measured with eddy-covariance (H_{EC}) for the southern and northern sites, respectively. For the southern site, linear regression (forced trough the origin) yields (W m^{-2}): $H_{LAS\_S} = 0.95H_{EC\_S}$, $R^2 = 0.89$ and RMSD = 24 W m^{-2}, and $H_{LAS\_N} = H_{EC\_N}$, $R^2 = 0.74$ and RMSD = 27 W m^{-2} for the northern site. The contrast between the two sites in terms of water availability (irrigation) can clearly be seen in these figures. Sensible heat flux values over the southern site are considerably higher than those over the northern site. In the southern site, the maximum value of H was around 300 W m^{-2}, while for the northern site the maximum was around 200 W m^{-2}. The comparison shows a better agreement for the southern site than for the northern site. There are several explanations for the scatter in Figs. 4a and 4b. During some of the intervals used in this study, conditions were partly cloudy. Additionally, an irrigation event had taken place just before the experiment, with irrigation reaching the location of the EC-system on DOY 291. This caused heterogeneity in terms of soil moisture in the northern site during the experimental period. The impact of this heterogeneity is amplified by the differences in the source area of

the LAS and that of the EC system. Indeed, due to the flood irrigation method employed in the site, it takes approximately 15 days to irrigate the entire field. During this period, the source area of the EC might be wet (dry) while a significant portion of that of the LAS is dry (wet).

Grid scale

In order to derive fluxes from LAS one has to rely on the Monin–Obukhov similarity theory (MOST). Since MOST requires horizontal homogeneity, the question is whether this theory still applies under heterogeneous conditions. Additionally, the measurements should be made above the blending height, which depends according to Wieringa (1986) on the friction velocity, wind speed and the horizontal length scale of the heterogeneities. Under the prevailing conditions over our study site, the average blending height was at about 26 m at the grid scale. Unfortunately, the operational deployment of the instruments at such height is not feasible. It is therefore of interest to investigate whether MOST holds under conditions of horizontal heterogeneity (at grid scale) where the measurements are made below the blending height.

$\langle C^2_{nLAS}\rangle_{agg}$ has been obtained assuming the linearity of scalars fluxes derived from the LAS (sensible heat and momentum fluxes over each field) using Eq. (11). In contrast to Lagouarde et al. (2002), who simulated values of $\langle C^2_n\rangle$ over a two-surface composite landscape by weighting values of C^2_n computed for each field from the sensible heat flux (eddy-covariance) according to the scintillometer weighting function, here $\langle C^2_{nLAS}\rangle_{agg}$ was directly derived using C^2_n from the LAS using Eq. (11) so that the non-linearity of C^2_n is avoided in the calculation of $\langle C^2_{nLAS}\rangle_{agg}$.

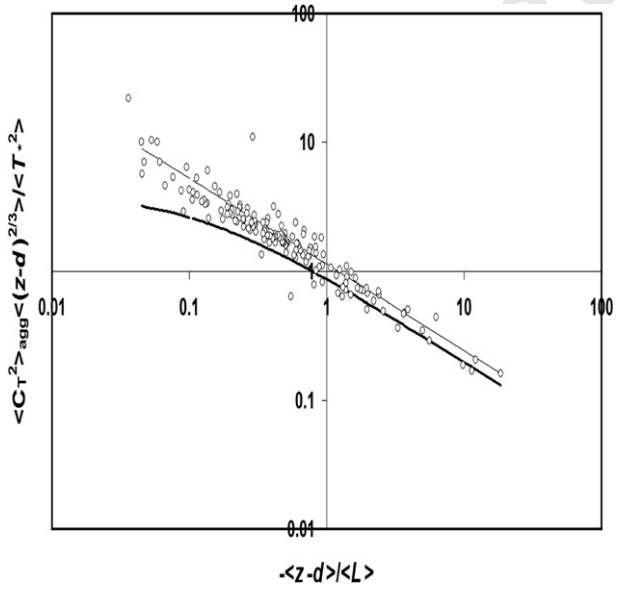

Figure 5 $(\langle C^2_T\rangle\langle z-d\rangle^{2/3}/\langle T^*\rangle^2)$ plotted against $-\langle z-d\rangle/\langle L\rangle$ during unstable conditions. Thick solid line represents the unstable scaling function found by de Bruin et al. (1993); also shown is the free convection relationship found by de Bruin et al. (1993): $f((z-d)/L) = 1.13(-(z-d)/L)^{-2/3}$ (solid line).

To check whether $\langle C^2_{TLAS}\rangle_{agg}$, calculated from $\langle C^2_{nLAS}\rangle_{agg}$ using Eq. (1), behaves according to MOST, we present in Fig. 5 a cross plot of $\langle C^2_{TLAS}\rangle_{agg}\langle z-d\rangle^{2/3}/\langle T_*\rangle^2$ and $\langle z-d\rangle/\langle L\rangle$. In order to avoid self-correlation due to MOST already being taken into account during the iterative procedure (Eqs. (1)–(5)), the effective values of $\langle\beta\rangle$, $\langle T_*\rangle$ and $\langle L\rangle$ have been constructed using solely eddy-covariance measurements. The result shows that the MOST scaling reported by de Bruin et al. (1993) still holds for heterogeneous surfaces, even though a small overestimation can be observed. Similar results have been found by Meijninger et al. (2002), who used the same scaling. These results confirm that MOST can be used below the blending height. This finding is in agreement with other studies (Shuttleworth, 1988; de Bruin, 1989; Ronda and de Bruin, 1999) which have shown that for surfaces with disorganized heterogeneity there is a layer below the blending height where MOST applies, but where contributions from separate fields can still be ''seen''. In the same vein, Kohsiek et al. (2002) reported that when deploying the XLAS (extra large aperture scintillometer, which can be used over pathlengths of up to 10 km) below the blending, the violation of MOST is negligible. This is of interest since the operational deployment of an XLAS over a distance up of 10 km at or above the blending height is just not feasible.

Since both EC systems have been installed at approximately the same height above the canopy, it is safe to assume that each EC system has a similar sized source area, and therefore $f_{iEC} = 0.5$ in Eq. (6). For the LAS however, since the two scintillometers are not set up with the same orientation, depending on the wind direction, large differences can occur between the dimensions of the source area of each LAS. Therefore, the effect of changing of f_c on the aggregation model has been investigated by varying f_c between 0.1 and 0.9. Statistical results for a comparison between $\langle C^2_{nLAS}\rangle_{agg}$ and $\langle C^2_{nEC}\rangle_{eff}$, in order to check the sensitivity to the composition of the surface on $\langle C^2_{nLAS}\rangle_{agg}$, are presented in Table 1. It shows that for the experimental site, to a good approximation, $f_c = 0.5$. In Fig. 6, a comparison between $\langle C^2_{nLAS}\rangle_{agg}$ and $\langle C^2_{nEC}\rangle_{eff}$ with $f_c = 0.5$ for cloud free days is presented. The comparison is good, with $R^2 = 0.95$ and the RMSD = 5×10^{-15} m$^{-2/3}$. Note that the difference between the statistical results for $f_c = 0.5$ as shown in Table 1 and in Fig. 6 is caused by the exclusion of cloudy intervals in the data used in Fig. 6.

Finally, in Fig. 7 the grid scale sensible heat flux ($\langle H_{LAS}\rangle_{agg}$) simulated from $\langle C^2_{nLAS}\rangle_{agg}$ (using Eqs. (1)–(5)) is compared with the area-average sensible heat fluxes $\langle H_{EC}\rangle_W$ defined as the linear weighing of sensible heat fluxes observed by the EC-systems of both fields with $f_c = f_{iEC} = 0.5$. The linear regression (forced trough the origin) yields $\langle H_{LAS}\rangle_{agg} = \langle H_{EC}\rangle_W$, $R^2 = 0.89$ and RMSD = 20.3 W m^{-2}. This result shows less scatter than the comparison at patch scale, and correlation is good.

In the present experimental setup, no third scintillometer has been installed over the two patches (and above the blending height) for validation. Besides practical constraints, it should be noted that it is practically impossible to have a source area that matches the ensemble of the source areas of the two LAS installed at the individual patches. This scintillometer would have a varying contribution of the southern and northern sites, depending on wind

Please cite this article in press as: Ezzahar, J et al., On the application of scintillometry ..., J Hydrol. (2006), doi:10.1016/j.jhydrol.2006.10.027

Table 1 Statistical results of the linear regression (forced trough the origin) between simulated effective grid average $\langle C^2_{n\ LAS}\rangle_{agg}$ with f_c (the fraction of the source area of LAS_S in the entire grid surface) varying between 0.1 and 0.9, and $\langle C^2_{nEC}\rangle_{eff}$ with $f_{iEC} = 0.5$

Portion of south surface (f_c)	Slope	Correlation coefficient	RMSD $\times 10^{15}$ ($m^{-2/3}$)
0.1	0.77	0.8	12.8
0.2	0.83	0.83	10.8
0.3	0.89	0.85	9.1
0.4	0.95	0.87	8.2
0.5	1	0.88	7.8
0.6	1.07	0.88	8.78
0.7	1.14	0.87	10.6
0.8	1.2	0.87	13
0.9	1.27	0.86	16

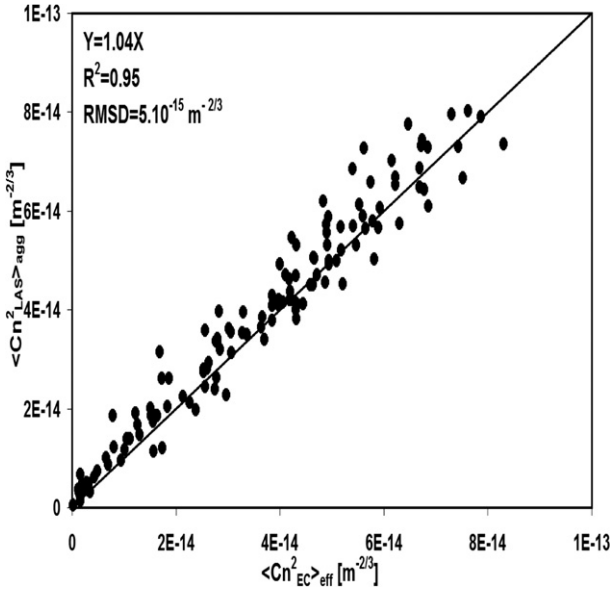

Figure 6 Comparison of $\langle C^2_{n_{LAS}}\rangle_{agg}$ obtained from the aggregation model and $\langle C^2_{nEC}\rangle_{eff}$ obtained from $\langle H_{EC}\rangle_W$, $\langle LvE_{EC}\rangle_W$ and $\langle L_{EC}\rangle$; intervals without cloud passes.

direction, which will differ considerably from f_c. Therefore, a third LAS does not provide a measurement that can be used to validate the aggregation method developed in this study.

Summary and conclusions

The general objective of the present study is to investigate the applicability of MOST at grid scale (i.e., the combination of the several individual fields, or patches). This is done by combining the LAS measurements over two individual patches with an aggregation scheme to infer the grid averaged refractive index structure parameter $\langle C^2_n\rangle$.

The comparisons between the half-hourly sensible heat fluxes obtained from eddy-covariance and LAS at patch scale yield a good result. The RMSD is 24.5 and 28.3 W m^{-2} for the southern and northern sites, respectively. The difference in flux between the two fields is mainly caused by an irrigation event which took place in the northern site during the experiment. This also explains part of the scatter and lower correlation between H_{EC} and H_{LAS} for the northern site, since during irrigation, the impact of the differences in the source areas of the two instruments increased significantly. However, despite some scatter, it can be assumed that MOST is applicable over relatively tall and sparse trees. Furthermore, the two comparisons show the difference between the two sites at the time of the experiment. Consequently, the grid, comprised of the two patches, can be considered as heterogeneous.

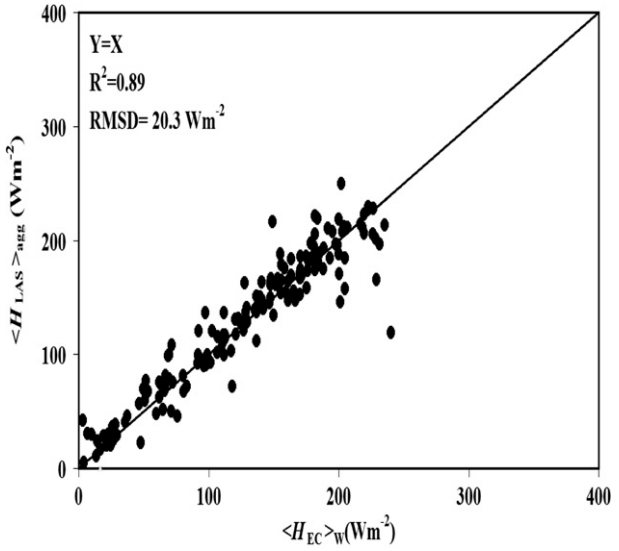

Figure 7 Comparison of grid scale sensible heat flux $\langle H_{LAS}\rangle_{agg}$ simulated from $\langle C^2_{n_{LAS}}\rangle_{agg}$ and $\langle H_{EC}\rangle_W$ derived by weighing the sensible heat fluxes observed from the EC-systems of both fields ($f_c = f_{iEC} = 0.5$).

A combination of patch scale LAS measurements, meteorological data and an aggregation model have been used to derive a grid averaged $\langle C^2_{nLAS}\rangle_{agg}$, from which the grid averaged structure parameter of temperature is calculated. This $\langle C^2_{TLAS}\rangle_{agg}$ is shown to behave according to MOST, although some scatter is observed. However, this scatter can be considered acceptable (see for example Beljaars et al., 1983; Weaver, 1990; de Bruin et al., 1993), and therefore MOST is considered to be applicable at grid scale, even when the measurements have been taken below the blending height.

There are practical constraints for the installation of a third scintillometer to measure over the entire grid; to overcome saturation and to be above the blending height (see for example Meijninger et al., 2002), one would have to install this third scintillometer much higher than the two LAS in used in this study. Therefore, in order to verify the accuracy of the values of $\langle C^2_{nLAS}\rangle_{agg}$, an effective parameter has been used. This effective approach uses averages of friction velocity and sensible and latent heat fluxes from the EC system in combination with MOST to calculate $\langle C^2_n\rangle$ values. In the case where MOST is applicable, this would be the grid-scale value of C^2_n, and this $\langle C^2_n\rangle_{eff}$ can therefore be used to

validate $\langle C^2_{nLAS} \rangle_{agg}$. Despite some scatter, the comparison is good which confirms the consistency of the aggregation method.

The results of this study demonstrate the applicability of the LAS and thus the XLAS, over large and heterogeneous grids when deployed below the blending height. Consequently, the minimum height at which a scintillometer can be operated is not the blending height, but the height below which saturation of the signal occurs (see for example Moene et al., 2005). Furthermore, since available energy is easily obtained from spaceborne sensors, e.g. Meteosat Second Generation or MODIS (http://postel.obs-mip.fr/postel/), this allows the determination of evapotranspiration at the aforementioned scales, which can be used for e.g irrigation monitoring, or the validation of mesoscale atmospheric models or hydrological models.

Acknowledgements

This research was situated within the framework of SUDMED, U.E. funded IRRIMED (http://www.irrimed.org) and Pleiades projects. We are grateful to the Institut de Recherche pour le Développement (IRD, France), the Department of Meteorology and Air Quality of Wageningen University (The Netherlands) and the PNTS (Programme National de Télédétection Spatiale, France). We are indebted to the director and staff of the Agdal olive orchard for access and use of the field site and for assistance with irrigation scheduling and security. Many thanks to O.K. Hartogensis for his technical assistance during the field experiment, especially on the preparation of the experiment and the installation of the EC-systems. During the experiment, J.C.B. Hoedjes was supported by a fellowship from STW, The Netherlands (project no. WMO4133).

References

Arain, A.M., Michaud, J.D., Shuttleworth, W.J., Dolman, A.J., 1996. Testing of vegetation parameter aggregation rules applicable to the biosphere–atmosphere transfer scheme (BATS) at the FIFE site. J. Hydrol. 177, 1–22.

Beljaars, A.C.M., Schotanus, P., Nieuwstadt, F.T.M., 1983. Surface layer similarity under nonuniform fetch conditions. J. Clim. Appl. Meteorol. 22, 1800–1810.

Beyrich, F., de Bruin, H.A.R., Meijninger, W.M.L., Schipper, J.W., Lohse, H., 2002. Results from one-year continuous operation of a large aperture scintillometer over a heterogeneous land surface. Boundary-Layer Meteorol. 105, 85–97.

Chehbouni, A., Escadafal, R., Dedieu, G., Errouane, S., Boulet, G., Duchemin, B., Mougenot, B., Simonneaux, V., Seghieri, J., Timouk, F., 2003. A multidisciplinary program for assessing the sustainability of water resources in semi-arid basin in Morocco: SUDMED. EGS-AGU-EUG Joint Assembly, April 6–11, 2003, Nice (France).

Chehbouni, A., Watts, C., Kerr, Y.H., Dedieu, G., Rodriguez, J.-C., Santiago, F., Cayrol, P., Boulet, G., Goodrich, D.C., 2000a. Methods to aggregate turbulent fluxes over heterogeneous surfaces: application to SALSA data set in Mexico. Agric. Forest Meteorol. 105, 133–144.

Chehbouni, A., Watts, C., Lagouarde, J.-P., Kerr, Y.H., Rodriguez, J.-C., Bonnefond, J.-M., Santiago, F., Dedieu, G., Goodrich, D.C., Unkrich, C., 2000b. Estimation of heat fluxes and momentum fluxes over complex terrain using a large aperture scintillometer. Agric. Forest Meteorol. 105, 215–226.

Chehbouni, A., Kerr, Y.H., Watts, C., Hartogensis, O.K., Goodrich, D.C., Scott, R., Schieldge, J., Lee, K., Shuttleworth, W.J., Dedieu, G., de Bruin, H.A.R., 1999. Estimation of area-average sensible heat flux using a large aperture scintillometer. Water Resour. Res. 35, 215–226.

Chehbouni, A., Njoku, E.G., Lhomme, J.-P., Kerr, Y.H., 1995. An approach for averaging surface temperature and surface fluxes over heterogeneous surfaces. J. Climate 5, 1386–1393.

de Bruin, H.A.R., van den Hurk, B.J.J.M., Kohsiek, W., 1995. The scintillation method tested over a dry vineyard area. Boundary-Layer Meteorol. 76, 25–40.

de Bruin, H.A.R., Kohsiek, W., van den Hurk, B.J.J.M., 1993. A verification of some methods to determine the fluxes of momentum, sensible heat and water vapour using standard deviation and structure parameter of scalar meteorological quantities. Boundary-Layer Meteorol. 76, 25–40.

de Bruin, H.A.R., 1989. Physical aspects of the planetary boundary layer with special reference to regional evapotranspiration. In: Proc. Workshop on the Estimation of Areal Evapotranspiration, Vancouver, BC, August, 1987. IAHS Publ., 177, pp. 117–132.

Green, A.E., McAneney, K.J., Astill, M.S., 1994. Surface layer scintillation measurements of daytime heat and momentum fluxes. Boundary-Layer Meteorol. 68, 357–373.

Hoedjes, J.C.B., Zuurbier, R.M., Watts, C.J., 2002. Large aperture scintillometer used over a homogeneous irrigated area, partly affected by regional advection. Boundary-Layer Meteorol. 105, 99–117.

Kohsiek, W., Meijninger, W.M.L., Moene, A.F., Heusinkveld, B.G., Hartogensis, O.K., Hillen, W.C.A.M., de Bruin, H.A.R., 2002. An extra large aperture scintillometer (XLAS) with a 9.8 km path length. Boundary-Layer Meteorol. 105, 119–127.

Lagouarde, J.-P., Bonnefond, J.-M., Kerr, Y.H., McAneney, K.J., Irvine, M., 2002. Integrated sensible heat flux measurements of a two-surface composite landscape using scintillometry. Boundary-Layer Meteorol. 105, 5–35.

Meijninger, W.M.L., de Bruin, H.A.R., 2000. The sensible heat flux over irrigated area in western Turkey determined with a large aperture scintillometer. J. Hydrol. 229, 42–49.

Meijninger, W.M.L., Hartogensis, O.K., Kohsiek, W., Hoedjes, J.C.B., Zuurbier, R.M., de Bruin, H.A.R., 2002. Determination of area-averaged sensible heat fluxes with a large aperture scintillometer over a heterogeneous surface – Flevoland field experiment. Boundary-Layer Meteorol. 105, 37–62.

Moene, A.F., 2003. Effects of water vapour on the structure parameter of the refractive index for near-infrared radiation. Boundary-Layer Meteorol. 107, 635–653.

Moene, A.F., Meijninger, W.M.L, Hartogensis, O.K., Kohsiek, W., de Bruin, H.A.R., 2005. A review of the relationships describing the signal of a Large Aperture Scintillometer. Internal Report 2004/2, Updated Version 1.1, Meteorology and Air Quality Group, Wageningen University, Wageningen, The Netherlands, 39pp.

Moore, C.J., 1986. Frequency response corrections for eddy-correlation systems. Boundary-Layer Meteorol. 37, 17–35.

Noilhan, J., Lacarrere, L., 1995. GCM grid scale evaporation from mesoscale modelling: a method based on parameter aggregation tested for clear days of Hapex-Mobilhy. J. Climate 8, 206–223.

Ochs, G.R., Wilson, J.J., 1993. A second-generation large-aperture scintillometer. NOAA Tech. Memo, ERL WPL-232, NOAA Environmental Research Laboratories, Boulder, CO, 24pp.

Panofsky, H.A., Dutton, J.A., 1984. Atmospheric Turbulence: Models and Methods for Engineering Applications. Wiley, New York, 397pp.

Ronda, R.J., de Bruin, H.A.R., 1999. A note on the concept of 'effective' bulk exchange coefficients for determination of surface flux densities. Boundary-Layer Meteorol. 93, 155–162.

Scott, R.W.C., Garatuza-Payan, J., Edwards, E., Goodrich, D.C., Williams, D.G., Shuttleworth, W.J., 2003. The understory and overstory partitioning of energy and water fluxes in an open canopy, semi-arid woodland. Agric. Forest Meteorol. 114, 127–139.

Shuttleworth, W.J., 1991. The modellion concept. Rev. Geophys. 29, 585–606.

Shuttleworth, W.J., 1988. Macrohydrology – The new challenge for process hydrology. J. Hydrol. 100, 31–56.

Twine, T.E., Kustas, W.P., Norman, J.M., Cook, D.R., Houser, P.R., Meyers, T.P., Prueger, J.H., Starks, P.J., Wesely, M.L., 2000. Correcting eddy-covariance flux underestimates over a grassland. Agric. Forest Meteorol. 103, 279–300.

Testi, L., Villalobos, F.J., Orgaz, F., 2003. Evapotranspiration of a young irrigated olive orchard in southern Spain. Agric. Forest Meteorol. 121, 1–18.

Wang, T., Ochs, G.R., Clifford, S.F., 1978. A saturation resistant optical scintillometer to measure C_n^2. J. Opt. Soc. Am. 68, 334–338.

Weaver, H.L., 1990. Temperature and humidity flux-variance relations determined by one-dimensional eddy correlations. Boundary-Layer Meteorol. 53, 77–91.

Webb, E.K., Pearman, G.I., Leuning, R., 1980. Correction of flux measurements for density effects due to heat and water vapor transfer. Quart. J. Roy. Meteorol. Soc. 106, 85–100.

Wesely, M.L., 1976. The combined effect of temperature and humidity fluctuations on refractive index. J. Appl. Meteorol. 15, 43–49.

Wieringa, J., 1986. Roughness dependent geographical interpolation of surface wind speed averages. Quart. J. Roy. Meteorol. Soc. 112, 867–889.

Please cite this article in press as: Ezzahar, J et al., On the application of scintillometry ..., J Hydrol. (2006), doi:10.1016/j.jhydrol.2006.10.027